scientific reports

Check for updates

OPEN

Machine learning based approach for surface roughness prediction in precision dental prototyping

Anmol Sharma[1,8], Ravinder S. Saini[2,8], Ashish Kaushik[3], Abdulmajeed Okshah[4], Mohamed Saheer Kuruniyan[2], Vishwanath Gurumurthy[2], Rajesh Vyas[4], Rayan Ibrahim H. Binduhayyim[2] & Artak Heboyan[5,6,7]✉

Complex geometries achievable with resin-based 3D printing are susceptible to lower levels of surface roughness, particularly in areas where support structures are attached and removed. The slicing parameter serves as the cornerstone for developing a model for predicting the corresponding output. In the present research, a resin 3D printer is used to fabricate the specimens in accordance with the combination of important parameters that were recovered utilizing the design of the experiment (DoE). Layer thickness, infill population density, print angle, exposure time, and lift speed are the five factors used to build DoE, which consists of 32 ideal runs for assessing surface roughness (SR). SR is a critical factor that influences the durability and effectiveness of dental devices. In order to anticipate output, a model is developed. To choose the best modelling strategies, a comparison of three base model techniques, artificial neural networks (ANN), support-vector regression (SVR), and decision trees (DT), as well as two ensemble techniques, random forest (RF) and XGboost, is conducted. This work utilized hyperparameter tuning for model improvement and use RMSE and R^2 as performance metrices for model efficiency. This application is still relatively underrepresented in the literature and often with isolated ML models rather than hybrid approaches. Among the three base models, SVR performs best with R^2 and RMSE 0.96745 and 0.017974 at C = 5 and gamma = 1 resp. Ensemble techniques justifying clubbing perform better in all ways with XGboost showing R^2 0.99858 and RMSE 0.00346998 as the best among all techniques. This work helps dental professionals in utilizing ensemble ML to improve model efficiency and predictability.

Keywords Additive manufacturing, Resin, Process modelling, Hyperparameter tuning

3D printing (3DP) advancements have paved new ways in the creation of patient-specific dental devices[1], allowing clinicians to customize appliances based on unique digital scans which ensures better fit and treatment outcomes[2–4]. In dentistry, 3D printing offers a significant shift from established, relatively slow-paced, and labor-intensive methods that often tend to miscalculations[3,5]. By providing a more efficient, precise, and reliable production method, 3D printing enhances the accuracy and quality of dental devices, ultimately improving patient care[6]. Despite its numerous benefits, 3D printing efficiency in dental applications is significantly impacted by surface roughness (SR)[1,7]. SR is a critical property of dental prostheses as it can promote bacterial adhesion and biofilm formation, leading to potential clinical complications[8,9].SR in 3D printing is influenced by several process parameters defined during the slicing process, such as infill density, light intensity, layer thickness etc[10]. Machine learning plays an important role in developing model that helps in predicting SR. The efficiency of model is explained using two performance characteristics RMSE and R^2. It also aids in recognizing basically about all the well-known individual and aggregation ML algorithms and the conditions under which they should be chosen while designing a reliable modell.

[1]USICT, Guru Gobind Singh Indraprastha University, Sector 16C, Dwarka, Delhi, India. [2]Department of Allied Dental Health Sciences COAMS, King Khalid University, Abha, Saudi Arabia. [3]Mechanical Engineering Department, Shree Guru Gobind Singh Tricentenary University, Chandu-Budhera Road, Gurugram, India. [4]Department of Dental Technology, COAMS, King Khalid University, Abha, Saudi Arabia. [5]Department of Research Analytics, Saveetha Dental College and Hospitals, Saveetha Institute of Medical and Technical Sciences, Saveetha University, Chennai, India. [6]Department of Prosthodontics, Faculty of Stomatology, Yerevan State Medical University after Mkhitar Heratsi, Yerevan, Armenia. [7]Department of Prosthodontics, School of Dentistry, Tehran University of Medical Sciences, Tehran, Iran. [8]Anmol Sharma and Ravinder S. Saini contributed equally to this work. ✉email: a_heboyan@farabi.tums.ac.ir

Resin is widely used when it comes to the fabrication of dental devices because of the following reasons owing to accuracy in fabrication, flexibility in use and customization[8,11,12]. However, in its nature, it gives some drawbacks in terms of surface characteristics, ending up to troubles such as microbial adhesion and discoloration, which are unfavorable particularly in dental prostheses[12–14]. To this end, polished denture bases are required in order to minimize microbial attachment and improve polish ability[15,16]. Additionally, denture base resins with good abrasion resistance are vital as they provide durability against mechanical wear from brushing and chewing[9,17]. On the other hand, resins with poor abrasion resistance can suffer from increased SR, which not only affects the appearance but also promotes crack propagation and dimensional changes, compromising the strength and longevity of the dental device[9,17]. Therefore, choosing base material with desired surface properties is essential to ensure durability and aesthetic appeal, even when using advanced digital fabrication technologies like 3D printing[18]. Compared to traditional methods, 3D printing in dentistry offers rapid production, high precision, and customization, making it easier to produce dentures and implant dental devices[19–22]. It reduces costs, provides personalized devices, and simplifies the workflow of dental appliance production[5,23,24].

Due to their accuracy and efficiency, the use of digital light processing (DLP), stereolithography (SLA), and LCD are the main 3D printing technologies propelling developments in resin dental 3D printing[6,25,26]. However, due to drawbacks such as poorer resolution, inappropriate material properties, or complicated processing requirements, other technologies such as fused deposition modelling (FDM), selectively laser sintering (SLS), selective laser melting (SLM), photopolymer jetting, and powder binder printing are less frequently utilized in dentistry[2,4,27–30].

The process of resin dental device printing involves several critical steps, starting with the selection of an appropriate 3D printing technology for its precision and effectiveness[31,32]. This is followed by setting optimal printing parameters to ensure accuracy and quality[33–35]. Here, the digital model is sliced into layers, guiding the 3D printer in the build process[7,33,36–38]. Later, post-processing steps, including cleaning, curing, and finishing, are essential to achieve the final functional and aesthetic properties of the dental device[39–41]. Each phase, from technology selection to post-processing, is meticulously controlled to produce high-quality, customized dental appliances[41,42]. Process parameters like print orientation, layer thickness, support structures, positioning, and alignment significantly impact the mechanical properties and accuracy of 3D-printed objects during fabrication[43]. Proper optimization of these parameters ensures strong, precise, and durable prints[33,44–47]. For enhanced aesthetics, color stability, and reduced toxicity, post-processing steps such as UV curing and isopropyl alcohol cleaning are crucial. These steps solidify and clean the object, ensuring complete polymerization and improving both functionality and appearance[14,18,44,48,49].Combining optimized in-process parameters with effective post-processing techniques results in high-quality, fully formed 3D printed products that meet both mechanical and aesthetic standards. One study explores the use of 3D printing technology to produce dental guides for dental treatment, analyzing dimensional aperture values with artificial neural networks (ANNs) with results demonstrating good accuracy rate of ANN in explaining data[50], stating ANN as an option to consider in work. The DL approach reduced calculation time by up to 1.5 times, improved print quality, reduced mean squared error (MSE), and identified new printing parameters. These results highlight DL's potential for broader application in 3D printing optimization, suggesting the need for further research into cost-effective and computationally efficient solutions in additive manufacturing[51]. This study reviews ANN advancements in 3D printing, highlighting challenges and potential solutions. Future trends suggest increasing ANN applications in 3D printing optimization[52]. This paper introduces a data fusion approach for predicting SR in 3D printing process, addressing the lack of studies in real-time monitoring and predictive modeling in additive manufacturing. Machine learning (ML) algorithms such as RFs, SVR, are employed to train predictive models integrated with a real-time monitoring system[53]. Experimental results show high accuracy in SR prediction, enhanced by the data fusion method[54]. Artificial intelligence (AI) has significantly impacted 3D printing, with various AI models and algorithms such as ANN, DT, and support vector techniques showing positive results. These advancements have led to improved process optimization, material property prediction, real-time monitoring, and quality control in manufacturing. Recent research in VAT photopolymerization has demonstrated the potential for creating complex material systems with adaptable properties, marking progress toward Industry 4.0. This review provides an overview of the evolution, current trends, and future prospects of computational AI models in 3D printing, highlighting their importance in driving technological advancements[55]. In this study, the ANN model was developed to predict the SR of 3D printed parts. The number of hidden layers and neurons significantly influenced the accuracy of the ANN[56]. This study aimed to develop a ML predictive model for dental diagnosis and treatment planning. It utilized four ML predictive models, concluding XGB algorithms showing the highest accuracy[57]. This study explores the use of ensemble ML algorithms to predict the mechanical strength of 3D-printed specimen. By varying process parameters such as ID, layer thickness, and employing algorithms like XGBoost, AdaBoost, and GradientBoost, predictive models were developed. The XGBoost ensemble model demonstrated the highest accuracy and lowest error metrics, suggesting its effectiveness in predicting material characteristics, showcasing ensemble technique benefits[58]. This study explores RF, AdaBoost, and XGBoost as learning methods to enhance Performance Factors Analysis (PFA) for predicting performance. Evaluation of three datasets demonstrates that XGBoost outperforms other models, significantly enhancing performance prediction compared to the original PFA algorithm[59]. Another study uses five ML algorithms to estimate raster angle, with RF outperforming others. This novel approach offers a reliable method to determine optimal results for improved material characteristics while reducing fabrication time and costs[46]. This review highlights the expanding role of 3D printing in healthcare, particularly dentistry, owing to its customization capabilities[60,61]. Surface roughness (SR) prediction using machine learning (ML) has been explored in prior studies, the novelty of our work lies in its specific context and approach, i.e., a comparative evaluation of basic and ensemble ML models on SR prediction for resin-based components fabricated via VAT photopolymerization (DLP-based) systems. This application is still relatively underrepresented in the literature. Most existing work focuses either

on FDM or SLA technologies, and often with isolated ML models rather than hybrid approaches. Also, the application focus on custom dental prototypes, where prediction reliability is critical for clinical acceptance and reproducibility. It is hypothesized that ensemble machine learning models outperform basic machine learning techniques in predicting the surface roughness of resin-based 3D-printed dental appliances due to their ability to reduce variance, mitigate overfitting, and enhance generalization across variable printing conditions. Furthermore, our methodology integrates RSM-based Central Composite Design (CCD) with machine learning, making it a hybrid experimental-modeling approach. This combination for optimizing SR in customized dental prototypes, particularly in a clinical fabrication context, has received limited attention.

This given work presents a framework for model optimization (MO) in accurately predicting output. The framework offers significant advantages in selecting effective methodology for optimizing model outcomes based on the design of experiments (DoE) and embracing ensemble-based optimization techniques for enhanced efficiency. It accommodates a wide range of process variables such as layer thickness, infill density, print angle, exposure duration, lift speed and objective SR, leveraging hyperparameter tuning for result improvement. The efficiency of the framework is demonstrated by utilizing two performance matrices, RMSE and R2, that played an important role in design processing.

Materials and methods

To explore the above-mentioned objective, the Response Surface Methodology (RSM) based technique has been used from DoE for five control factors which are Layer thickness, Infill density, print angle, Exposure duration and Lift speed and for one response variable which is Surface roughness. To optimize experimental efficiency without compromising model reliability, this work adopted a Central Composite Design (CCD) under the RSM framework, which generated 32 statistically optimized combinations. This method provides, Uniform coverage of the multidimensional design space, Controlled variation for accurate model fitting, And significant reduction in experimental load and cost. All in all, thirty-two input parametric combinations are discovered as displayed in Table 1 below. This means that each data set that is generated refers to one exact string of parameter values. While it may appear that the dataset contains near-duplicate observations, it is important to emphasize that the data points are generated through a structured Design of Experiments (DoE) approach, specifically using Central Composite Design (CCD). In such experimental designs, the input parameter combinations may be numerically close but are purposefully selected to capture curvature and interaction effects in the response surface. These are not duplicates but strategically designed data points to reflect the design space adequately. Some near-replicate configurations are embedded within DoE as part of its characteristics to assess curvature effects, check for interaction terms, and enhance the generalizability of the model. These structured variations are not redundancies but essential design features that help ensure robust statistical modeling. These test specimens are printed for SR evaluation but in accordance with the specifications provided in ASTM D695. For the preparation of the test samples, a resin 3D printer is used. For the body of the test samples, a resin material has been utilized. It is a methacrylate based resin which is a subgroup of photopolymer resin and it is commonly used in the medical field due to its high tear strength, feasible viscosity around 700centipoise and biocompatibility making it a suitable choice for dental device fabrication.Viscosity plays a vital role in vat photopolymerization-based additive manufacturing, particularly when high surface accuracy and layer uniformity are required for dental applications. This study employed a resin with a viscosity of approximately 700 cP, which falls within a favorable range for dental printing tasks. To ensure optimal fabrication, a temperature-controlled environment is maintained to avoid unwanted fluctuations in resin viscosity that can affect layer recoating and photopolymerization uniformity. Also, a closed printing chamber helped prevent environmental disturbances (as such airflow, temperature shifts) that might otherwise lead to inconsistent resin flow or layer bonding and consistent and stable exposure and recoating conditions are monitored throughout the print job to support predictable and uniform curing. The initial installation of the design is done through Fusion 360 then adjusted into a printable format hence making input configuration for the 3D printer easy. The next process that is applied to a file in a printable format is the slicing process using the software module that cuts the model into layers of the set height. Other parameters such as layer thickness are set with the help of controls offered by the maker of the machine and then the printing process begins. As for each combination of parameters, test pieces of the resin material were produced with the help of the slicer software of the used resin printer, and then the mentioned values of SR were determined after preparing the test pieces. Figure 1 demonstrates the resin 3D printer used for the study. To reduce the toxicity and improve the general appearance of the specimens, the prints are first rinsed with 90% isopropyl alcohol for 5 min according to the manufacturer's prescription and then underwent curing for 30 and 60 min[48]. For post-curing, work conducted multi-stage trials at various exposure durations to identify a curing profile that achieves complete polymerization, dimensional stability, and optical clarity in the printed dental devices. This staged approach also helps reduce internal stresses and minimizes surface deformation, which is crucial for achieving a smooth and accurate finish. As indicated by the experimental results and especially by the visual analysis of the specimens, the samples that were treated with a curing time of 60 min evidenced the best results in terms of quality. Therefore, as a result of the above study, a curing time of 60 min was taken as the reference time in the subsequent specimens. For the rest of the remaining 31 specimens, the same experimental procedure was carried out with the control variables deliberately altered systematically with the purpose of observing a large portion of possible input combinations. After the manufacturing of samples and the subsequent curing process, SR is recorded for each of the specimens to enable the accumulation of data that would be subjected to analysis. In the current article, the interaction between the input parameters and SR is analyzed, and to do so RSM interaction model is used. These models form the basis of subsequent analysis as they unveil future assessments. The developed models are then incorporated with machine learning optimization algorithms.

Layer thickness	Exposure duration	Print angle	Infill density	Lift speed	Surface roughness
(mm)	(sec)	(degree)	(%)	(mm/sec)	(Microns)
X_1	X_2	X_3	X_4	X_5	Y
0.065	4	67	40	3.5	0.465
0.065	4	67	80	3.5	0.412
0.05	5.5	90	60	5	0.293
0.08	5.5	90	60	2	0.519
0.08	5.5	90	100	5	0.462
0.08	2.5	90	100	2	0.473
0.065	4	67	80	3.5	0.416
0.065	4	67	80	3.5	0.414
0.065	4	90	80	3.5	0.385
0.08	2.5	45	60	2	0.611
0.05	2.5	45	60	5	0.371
0.05	2.5	90	100	5	0.26
0.05	5.5	45	60	2	0.346
0.055	4	67	80	3.5	0.326
0.05	5.5	90	100	2	0.239
0.065	4	67	80	6.5	0.425
0.065	4	22	80	3.5	0.465
0.065	4	67	100	3.5	0.384
0.065	4	67	80	3.5	0.427
0.065	4	67	80	3.5	0.419
0.065	4	67	80	1.5	0.418
0.05	5.5	45	100	5	0.291
0.065	2	67	80	3.5	0.411
0.08	2.5	90	60	5	0.551
0.05	2.5	90	60	2	0.3
0.08	2.5	45	100	5	0.525
0.08	5.5	45	60	5	0.605
0.065	4	67	80	3.5	0.431
0.095	3.5	67	80	3.5	0.649
0.08	5.5	45	100	2	0.5
0.065	6.5	67	80	3.5	0.395
0.05	2.5	45	100	2	0.297

Table 1. RSM-based design of experiment with significant input parameters and corresponding output.

Experimental setup for measurement of surface roughness

Using the Surfcom hardness tester S130A, the Ra value of the 3D-printed specimen is evaluated. By measuring height changes on a surface, this device uses contact-based techniques. Using a stylus that comes into contact therewith the surface as its working principle, the SR tester conducts a linear scan in which changes in profiling height are captured as electrical impulses or signals, allowing the Ra value to be calculated. For a variety of applications in fields including manufacturing, engineering, and dentistry, the SR tester helps assess and guarantee the required surface quality by giving SR a numerical representation. Only 2D space, either vertically or horizontally, working around a reference surface, may be used to compute these measures. SR, graphically, corresponds to deviations in height relative to a reference plane. The procedure commences by preparing the specimen, securely mounting it on a stable surface to ensure accuracy in measurements. Calibration of the SR tester with a skidding probe is then conducted as per the manufacturer's instructions to establish a reference plane. To maintain consistency and reliability, the measurement speed is kept hold on 0.30 mm per second. After adjusting the measurement settings, the SR tester is brought into contact with the 3D-printed specimen, and the probe is moved linearly across its surface at a consistent pace. The device records continuous surface profile data, which is subsequently analyzed to finally provide R_a value. This standardized procedure ensures accurate and dependable SR measurements, facilitating the assessment of print quality and performance for 3D-printed objects. For better accuracy of R_a, measurement is performed three times and the average of three is used as the final output.

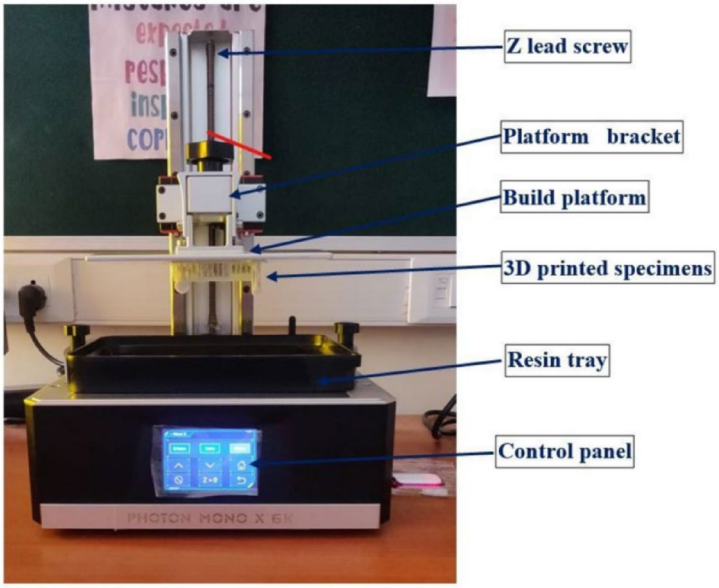

Fig. 1. Resin 3D printer used for specimen preparation[62].

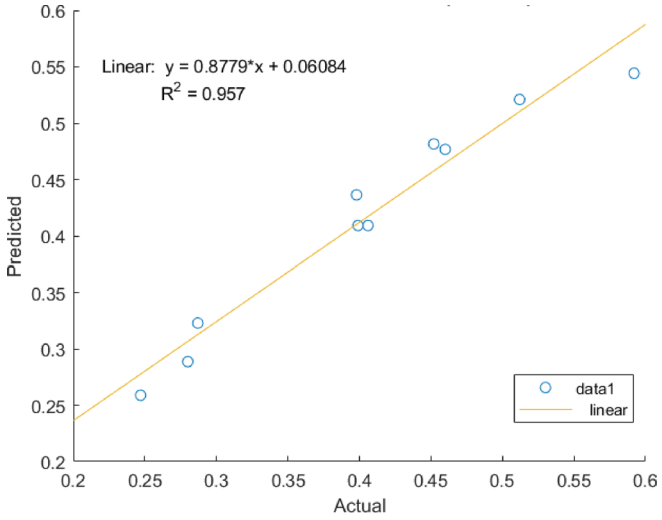

Fig. 2. Graph representing relation between actual and predicted results from ANN.

Modelling using basic model techniques

ANN

Neural networks are artificial, neurotically connected systems similar to biological neurons that are capable of learning[52]. They are well-adapted at automation with high-speed analytics using stored experimental data to accomplish tasks in recognizing patterns[63,64]. The backpropagation (BP) network was widely applied but it has some drawbacks[65]. Some can be utilized to forecast future results and drive the resolution of experiment design efficiently. ANN is one of the modelling techniques that imitates the human nervous system whereby learning takes place based on the sample data[66]. It learns from examples that are representative of natural occurrence of physical events or decision-making. As mentioned above, ANNs are particularly good at searching for regularities of relationships between independent and dependent variables and at solving complex data processing tasks without constructing event ontologies[52,67]. These are the considerations that allow them to work with noisy data proficiently Credit: Fig. 2 shows the graph. An ANN is mainly composed of the input layer, hidden layer and output layer[56]. Input nodes transmit information to hidden nodes through activation functions, while hidden nodes process this information based on weighted evidence. When a hidden node's value surpasses a threshold, it triggers output nodes[7,52]. ANNs require training with numerous cases to function effectively. However, they may struggle with unfamiliar or extreme events, lacking sufficient training data. In this work, an ANN model is constructed to predict the SR of resin specimens fabricated via a resin 3D printer. The model's input variables

include process parameters like LT, ID, ED, LS, and PA, while the target variable is the SR. Data is divided into training and testing sets. ANN training is achieved with the Levenberg-Marquardt algorithm which is a type of backpropagation algorithm characterized by memory efficiency as well as fast computation. Cross-validation is also used for evaluation and the assessment of the model is based on mean squared error (MSE). The Levenberg-Marquardt algorithm is hybrid in that it contains a combination of the gradient descent and the Gauss-Newton methods which are numerical algorithms for calculations. In ANN sigmoid transfer function is applied with the purpose of activation of weights. When splitting data, most of the time, 70% is used to train the model while 30% is used to assess the performance of the model.

As previously said, each layer's neurons get compensated donations from the previous layer and transfer them to the layer that follows.

$$Y_{net} = \sum {}^{n}_{i=0} X_i W_i + W_0 \tag{1}$$

calculates the weighted input signal total, which is then sent via the equation's nonlinear activation function[68].

$$Y = f\left(Y_{net}\right) = \frac{1}{1+e^{-x}} \tag{2}$$

The network error was then determined by MSE

$$\mathrm{MSE} = \frac{1}{k} \sum {}^{k}_{i=1} (Y_i - O_i)^2 \tag{3}$$

considering the relationship between the expected and actual results. In most cases, even after the preparation cycle is over, this inaccuracy achieves a satisfactory level[69].

$$var\left(y\right) = \mathrm{E}\left[Y^2\right] - E[Y]^2 \tag{4}$$

$$R^2 = 1 - \frac{MSE}{var\left(y\right)} \tag{5}$$

$$RMSE = \sqrt{\frac{1}{n}\left(\sum {}^{n}_{i=1} (x_i^{actual} - x_i^{predicted})^2\right)} \tag{6}$$

This division helps the model acquire the set of patterns from the sizeable number of examples during training and keep aside some for checking its performance of the new set of patterns it has not been trained with. Training and testing are perhaps the basic steps that are known in the context of ANN development. In the training process, the parameters of the model are updated step-by-step by using the training data in order to achieve minimum mean squared error. The testing procedure checks the model's effectiveness on data that have not been used in its training in order to determine how it will perform in general cases. The choice of the number of neurons and the hidden layers within an ANN is one of the significant factors that determines the accuracy of prediction[70]. The size and the depth of the networks together determine how effectively the architecture of the neural network can learn the complexity from the given data set. Finding the appropriate number of layers and nodes in a model and the sequences in which they are connected is vital to get high accuracy from the model. This work investigates the influence of neuron quantity and hidden layers on the accuracy of the neural network to predict the trend through the use of the R^2 value.

ANNs were initially inspired by the biological brain's computational capabilities but diverge significantly in architecture[55,71]. ANNs handle large, high-dimensional datasets through interconnected layers of nodes. The network typically consists of input, hidden, and output layers, with each layer containing interconnected nodes that process data through mathematical functions[55]. Nodes activate based on weighted inputs, transforming data as it progresses through the layers. Hidden layers, whose values are not directly specified by the training data, contribute to the network's ability to learn complex patterns. ANNs autonomously acquire and process information, making predictions without needing explicit mathematical definitions or extensive experimentation[54,67]. Table 2 depicts various ANN architecture performance, where P represents parameter, HL Hidden layer and N neurons. Figure 2 represents graph for ANN best performance metrices.

SVR

Support Vector Regression (SVR) is a type of supervised learning method that is suitable for regression analysis since the intent is to predict the continuous values for the dependent variable and intends to transform the input variables to dependent variables by constructing the mapping function, and at the same time, the generalization of the constructed machine learning model controls the total mathematical error within a fixed or tenable range[30]. This is realized by finding the maximum-margin hyperplane that satisfies the data points within a certain distance from the hyperplane and the support vectors are the data points closest to this hyperplane[72,73].

SVR is a regression algorithm that includes the fuzzy factor in the sense of margin of tolerance known as epsilon (ε), whose aim is to minimize errors while confining output to a certain margin[68,74,75]. The main idea of SVR presupposes the use of the so-called support vectors which are the points belonging to the area close to a hyperplane that defines the regression function. Its purpose is to compute a hyperplane (or more than one if the association is nonlinear) through the points that enable categorization to fall inside a margin of error[72,76]. Due to its analysed ability SVR employs the so-called kernel trick and transforms the input variables into the

ANN architecture (*P*-HL-*N*)	RMSE	R^2
5-1-2	0.10865	0.097357
5-2-6	0.095185	0.30727
5-1-1	**0.024013**	**0.95591**
5-2-7	0.096614	0.28631
5-1-10	0.10948	0.083548
5-5-7	0.088052	0.40721
5-4-1	0.063685	0.6899
5-5-3	0.071932	0.60439
5-1-5	0.067081	0.65594
5-2-3	0.10359	0.1796
5-3-4	0.092074	0.35181
5-2-5	0.10668	0.12982
5-5-8	0.10283	0.19157
5-4-4	0.12027	-0.10598
5-1-4	0.090416	0.37494
5-4-2	0.061301	0.71268
5-2-4	0.072604	0.59696

Table 2. ANN architecture variations and corresponding performance metrices. Best R^2 0.95591 and Best RMSE: 0.024013.

high-dimensional space[75,77]. It minimizes an objective function that caps the errors to a certain amount outside a margin and may use some kind of regularization to avoid over-fitting. While in training, SVR finds the support vectors as well as the hyperplane(s) that provide the best margin using methods of optimization[46,70,78].

$$y = (K_{xi} * W_{jk}) + b \tag{7}$$

SVR works by finding the optimal hyperplane(s) that fit the data within a specified margin of tolerance. It involves data preprocessing to ensure uniform scaling, followed by kernel selection, where non-linear relationships are addressed using kernel functions like the radial basis function here[73,77]. Model training aims to minimize error within the tolerance margin, with techniques like quadratic programming used for optimization. Epsilon defines the acceptable error range, and support vectors, closest to the hyperplane, influence the regression function. Finally, the model is evaluated using metrics like RMSE and R^2 to ensure optimal performance. SVR balances close data fitting with specified error tolerance, even in non-linear relationships.

If the kernel function is *Kxi*, then the SVM network's bias term is b. The weight vector is referred to as *Wjk*. Lagrange multipliers are indicated by *Kx* and *W*. An input vector is mapped to a high-dimensional feature space via the nonlinear function known as the *Kxi*. The following is one way to express the nonlinear function method's equation[46]:

$$K_{xi} = e^{-\gamma \|P_i - Y_i\|^2} \quad \gamma > 0 \; and \; i = 1, 2, 3, ?, n \tag{8}$$

In order to perform these steps, the following steps are followed in order to select the model with the lowest RMSE and the highest R2: First of all, divide the data set into the training and test sets. Then, proceed to the hyperparameter grid search where one adjusts C and gamma for the RBF kernel only. The best hyperparameters are those that provide the lowest value of RMSE and the highest R2. The following hyperparameters should be used in tuning a new SVR model on the entire training set: Finally, on the test set come to evaluate this model to obtain the final RMSE and R2 values. It was observed that the model with the low RMSE and the high R2 on the test set was the best model to select hence in Table 3 below, the best model is highlighted. This systematic approach makes it possible of arriving at the right SVR model to use in predicting the target variable on unseen data. Figure 3 shows the results of data correlation from SVR modelling.

In SVR, it is the regression function which lies within the margin of tolerance given 'epsilon'. It seeks to achieve a small difference between the model predicted values and the actual observations bearing in mind this margin of error. Margin is a distance to and from the hyperplane; Support vectors are the data points that lie in the vicinity of the hyperplane and constitute its reference points and the line or plane within which acceptable error lies. These play an important role in defining the hyperplane(s) and the number of parameters in the model, respectively. Essentials of SVR Besides, in the SVR model, only support vectors have non-zero coefficients, which is beneficial to improve the generality of the model.

Decision tree

Decision trees resemble flowcharts in structure, with terminal nodes signifying class names, branches displaying test results, and interior nodes representing test characteristics[79]. They're valuable for mapping decisions and their consequences, making predictions, and guiding material and process selection[80]. In 3D printing, where parameter correlations are complex, decision trees aid in predicting outcomes. They're widely used in decision-

C	Gamma	RMSE	R^2
1	1	0.018083	0.96706
3	4	0.043254	0.81151
2	3	0.041507	0.82643
3	3	0.040258	0.83672
5	4	0.042707	0.81625
1	4	0.043804	0.80668
4	4	0.042985	0.81384
4	3	0.039019	0.84661
5	5	0.043679	0.80779
1	3	0.042759	0.8158
2	2	0.027687	0.92277
3	2	0.021335	0.95414
4	5	0.043752	0.80714
5	5	0.043679	0.80779
2	5	0.043951	0.80538
1	5	0.048843	0.75965
5	3	0.037787	0.85615
4	2	0.018142	0.96684
5	**1**	**0.017974**	**0.96745**

Table 3. Hyperparameter tuning and their corresponding performance metrices for SVR. Best hyperparameter C = 5, Gamma = 1, RMSE = 0.017974 and $R^2 = 0.96745$.

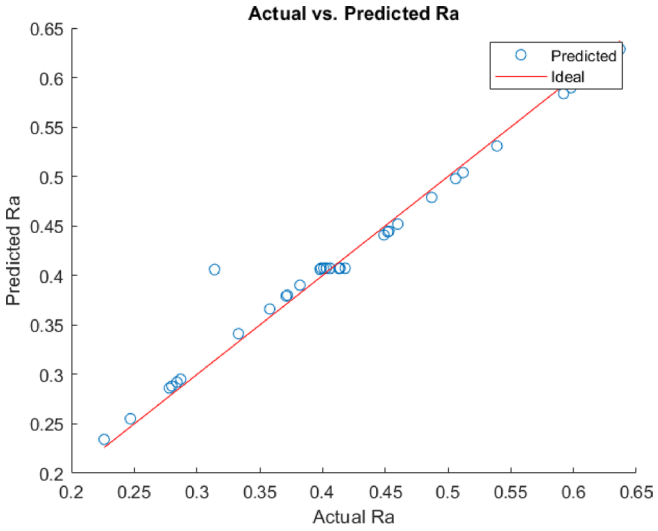

Fig. 3. Graph representing actual vs. predicted outcome variation from SVR.

making involving AI by constructing predictive trees[81]. Decision trees are utilized in 3D printing businesses to assist customers in material selection[82]. Decision tree regression (DTR) is a crucial technique for prediction[83]. It comprises a root node, internal nodes, and leaf protuberances, dividing sample space based on input attribute values[84]. Each internal node splits the space using input attributes subjected to specific functions, contributing to accurate modelling[46].

$$SDR = SD(T) - \sum \left|\frac{T_i}{T}\right| SD|T_i| \tag{9}$$

SDR: Standard Deviation Reduction.
SD(T): The standard deviation of the target variable before the split (for the parent node).
T: The entire dataset (or node) before the split.
T_i : The subset of the dataset after the split (the child node).
$SD(T_i)$: The standard deviation of the target variable within the child node T_i.

Depth	R^2	RMSE
1	0.84925	0.038682
2	0.82632	0.041519
3	0.82632	0.041519
4	0.82632	0.041519
5	0.82632	0.041519
6	0.82632	0.041519
7	0.82632	0.041519
8	0.82632	0.041519
9	0.82632	0.041519
10	0.025089	0.098371

Table 4. Table depicting performance metrices at various depths. Best R^2: 0.84925, RMSE: 0.038682.

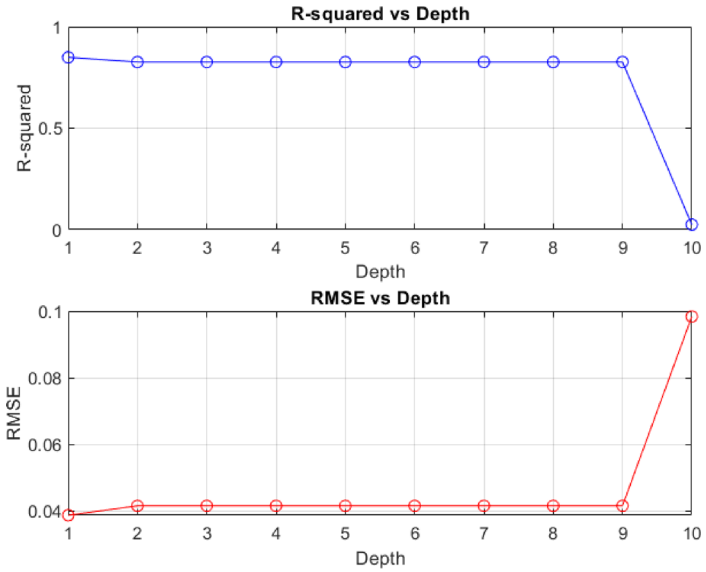

Fig. 4. Convergence of performance metrices at various depth of trees.

$\frac{|T_i|}{|T|}$: The proportion of instances that end up in child node T_i compared to the total instances in the parent node.

Starting at the root node, the algorithm moves up the tree according to the input feature values until it reaches a leaf node[85]. A projected output value is eventually reached at the leaf node after judgments are taken at each stage in accordance with the criteria established by the features[82]. Converging values data are shown in Table 4, and a graph is used to illustrate convergence in Fig. 4.

Modelling using ensemble techniques

Random forest

A popular ensemble learning technique in data mining and visualisation, Random Forest (RF) combines many decision trees for increased accuracy[82]. Thus, it might be used for both classification and regression problems when the forecasts are calculated as the mean of all the forecasts obtained with using all the generated trees[46]. RF is present in numerous fields and industries and is, therefore, under observation. For better performance and to predict the model for different setting with high conclusiveness, RF is generalized with other methods like NN, kNN and RR[83]. Random Forest Regression (RFR) builds several models of decision trees independently with different observation samples, which offers a good model[70]. The Random Forest Regression (RFR) algorithm is highly valued for its function to assess a database multiple model so deeply. Due to improved performance in both regression and classification issues, which is more time-efficient than other methods, this method has a more advantage[57]. In comparison with the RFM, RFR has a higher speed of prediction and fewer regularization parameters, thus making it more suitable for solving multidimensional problems. That is why, the RFR model reduces the degree of overfitting, which is characteristic of decision trees. This is done by building many separately developed decision trees where each tree is developed with random subsamples of observations and features from the training data sample. It involves the averages of the estimate of each tree in the regression terminologies[86]. The number of attributes randomly selected overall predictor variables at the nodes and the

number of trees within the canopy are the two key decision parameters of RFR. These are some of the parameters that were used to be sensitive in this model and improved to enhance the ability of the model to predict accurately.

A powerful learning method known as Random Forest is composed with decision trees that are constructed independently on random samples of features of the data[87]. Decision trees propose the partition of data in a manner that will facilitate the acquisition of more information, or minimization, on the other hand, of impurity based on a set of feature values. Random forest limits trees on the specific nodes because it guarantees tree diversity through the use of bootstrapping and selecting features at random. Thus, in regression, they predict numerations, which are numbers, and the last prognoses are the mode or average varieties[83]. To avoid overfitting, Random Forest uses bagging, where the model produces numerous trees, and the result is a projection of the average of all the trees obtained. Some of the hyperparameters include the number of trees that are to be generated and the depth of the trees, that is, the number of levels that a tree can possess, which can be tuned to improve the model's efficiency[88]. It also helps in determining the importance of the features, which can be useful for selecting the features or for understanding the pattern in the data set. One of the most used and highly reliable methods of machine learning, Random Forest can be applied to various domains such as finance and healthcare due to its high efficiency and easy implementation ability.

In a decision tree every node refers to a test that is made depending on a feature and the results are further predictions or forecasts. Decision trees are hierarchical structures. Random Forest is one of the assembled learning models that generates a number of decision trees utilizing bootstrap sampling and selecting random features. When only some of the characteristics are taken randomly throughout the split, the overfitting is minimized and the number of trees is maximized. Bagging is used just to derive a set of a number of decision trees, each of which minimizes variance and increases generalization. In order to fine-tune models, parameters, including the number of trees and trees' depth, should be most important and it can be done using such methods as the grid search or the random search. This provides an insight into the random forest and shows how decision trees, bootstrapping, ensemble learning, and tuning of hyperparameters are used to produce efficient machine learning models.

Tuning hyperparameters is a very important procedure to make Random Forest as efficient as possible. This process involves the selection of hyperparameters and provides some values to the parameters, such as estimators and adept. When it comes to the choice of an evaluation measure in regression analysis, an appropriate one, say RMSE and R2 is used. All the configuration of the six set parameters is worked out by the grid search method out of which the best configuration is selected out of it and graph is plotted in Fig. 5. In order to ensure that the results will be applicable to a more general real-world setting and show good performance in situations similar to those in 'real life', a final model with optimal hyperparameters has been trained on the entire dataset to make sure

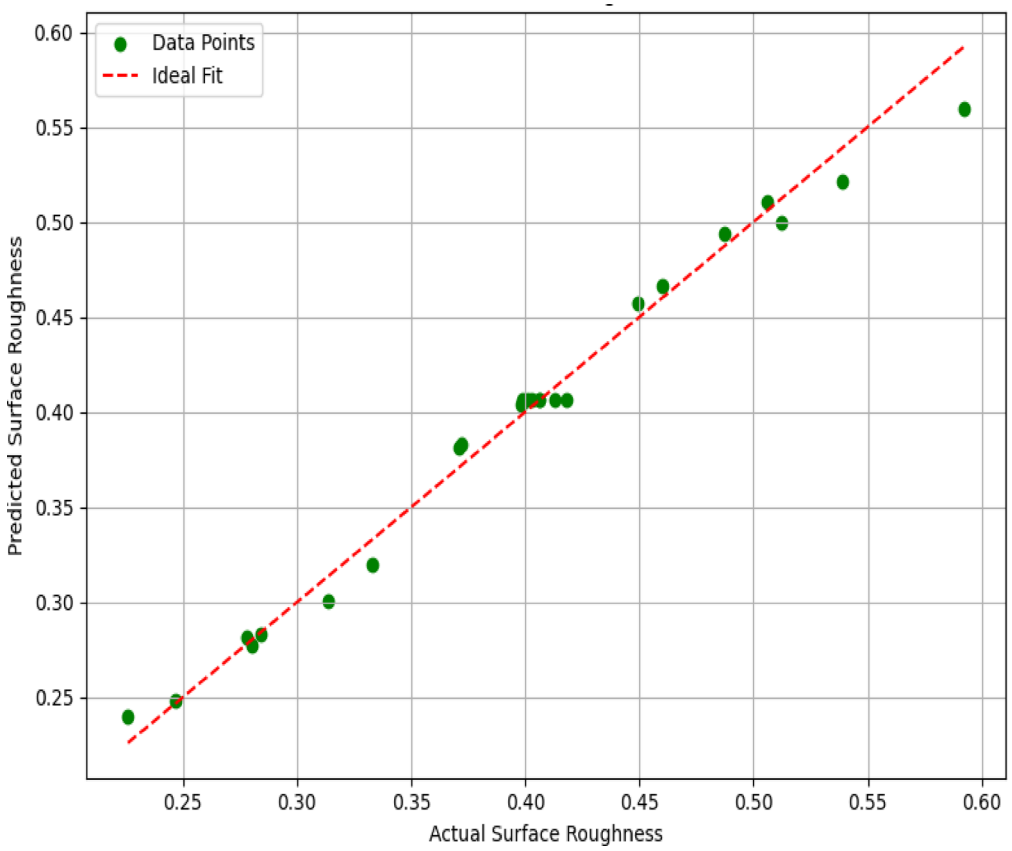

Fig. 5. Actual vs. predicted outcome fitting from Random forest modelling.

that it is adjusted for the chosen problem, and then evaluated on the test set. It also greatly enhances challenging circumstances when completing this methodology ensures that the applications are resistant and boosts model efficiency.

R^2: 0.9864165223734502, RMSE: 0.010734192405298678.

XGboost

XGBoost is an enhanced version of the Gradient Boosting algorithm also used for the construction of the models of the regression type of supervised machine learning[89]. Gradient boosting technique is a type of machine learning technique in which a model is built iteratively by adding further 'weak' models to the existing models[90]. XGBoost is known for two major attributes: great accuracy in the results and speedy computation; thus, XGboost is advisable to use for regression predictive modelling. As from different reviews, it is more accurate than other models and, in some sense, the time taken in order to run the model is shorter, especially when working with structured tabular data. Some of the components of XGBoost include base learners as well as the objectives that come with a penalty and that of a loss function[57]. It thus defines other variables' errors between the expected and actual results, which will assist the model in preventing errors[88]. The XGBoost also aids in establishing a number of base learners to increase the accuracy of prediction[58]. The aim of the method is to select base learners that will help in making better guesswork in the end by averting the resulting errors that may be done.

XGBoost is found to be better than other algorithms in terms of accuracy, training time, the interaction between the independent variable and the dependent variable, explaining the ability of the model and very few hyperparameters are to be tuned[88]. This is because, in a case where there is a relation in the variables used in the analysis, then the regression is capable of capturing nonlinear equations[59]. This makes it a preferred choice among researchers for predicting output variables based on input variables. XGBoost's interpretability is comparable to random forests, but it typically achieves higher predictive accuracy when properly trained with corresponding hyperparameters[87]. In manufacturing domains, XGBoost has been widely applied for various tasks. For instance, to develop a real-time Industry 4.0 customization framework, achieving synchronization between customer inputs and manufacturing process outputs, to predict geometry in additive manufacturing, demonstrating its superiority over artificial neural networks even with small datasets. In material science, where relationships between properties, compositions, and manufacturing parameters are complex, XGBoost has been utilized effectively[91].

XGBoost demonstrates superiority over other machine learning algorithms such as support vector machines and radial function models in various applications. In quality monitoring, XGBoost-based models effectively reinforce quality in machining operations. Additionally, XGBoost has been utilized for the prediction of material characteristics, yielding excellent coefficient of determination values. Despite its success in discrete manufacturing domains, its application for real-time machining data prediction, such as predicting SR remains limited[92]. The corresponding graph representing the best correlation is shown in Fig. 6.

R^2: 0.9985805264402483, RMSE: 0.0034699845680639147.

Results and discussion

In direct 3D printing for dental applications, precision and accuracy are vital for creating high-quality devices. This accuracy hinges on the efficiency of the model developed to predict the desired properties. This study employed various machine learning techniques, optimized through hyperparameter tuning, to enhance the model's efficiency in predicting SR. The ML algorithms used include three basic ANN, SVR, DT, and two ensemble techniques RF, and XGB. This performance analysis provides insights into why ensemble methods are superior and how hyperparameter tuning enhances model accuracy. DT Best Depth: 1, R^2: 0.84925, RMSE: 0.038682 A shallow decision tree with depth 1 captures the most significant split in the data, providing a baseline prediction. However, it lacks the complexity to model intricate patterns in SR, leading to lower accuracy compared to more advanced techniques. SVR best Hyperparameters: C = 5, Gamma = 1 R^2: 0.96745 RMSE: 0.017974 SVR utilizes kernel functions to handle non-linear relationships, making it robust against overfitting. The optimal combination of C and Gamma maximizes the margin between predicted and actual values, resulting in high predictive accuracy. However, SVR still falls short of ensemble methods due to the lack of robust error correction mechanisms. ANN Best architecture (5-1-1) 5 parameter 1 Hidden Layer, 1 Neuron givess R^2: 0.95591 RMSE: 0.024013 provides a good balance between model simplicity and predictive power. In contrast to ensemble approaches, this configuration's lack of depth and complexity restricts its capacity to capture more complicated patterns. RF combines many decision trees, each trained on distinct subsets of the data, yielding an R2 of 0.98641 and an RMSE of 0.0107341. High prediction accuracy is achieved by mitigating overfitting and reducing variation using an ensemble technique. Robustness and dependability are guaranteed by averaging the forecasts from several trees. With an R2 of 0.9985 and an RMSE of 0.00346, XGboost produces the greatest results since it creates models one after the other to fix the mistakes of earlier iterations, hence lowering bias and variance. Regularisation strategies in conjunction with this iterative refining help to improve generalization and avoid overfitting.

The second derivative of the cost function and parallelism increases the training efficiency and the general effectiveness of the training model. At the same time, ensemble methods such as, XGBoost and Random Forest use several weak learners and thus experience faster and more stable convergence rates. For instance, techniques like SVR and ANN, even though good performing models, do not possess the ability of error correction in an ensemble setup, thus leading to comparatively low accuracy. Random Forest eliminates the risk of overfitting an individual decision tree because it combines the forecasts of many such trees that are randomly generated. It successively constructs models that aim to fix mistakes of the former models minimizing both bias and variance. This makes the model to be more accurate and powerful. XGBoost uses boosting to successively try to correct mistakes in models which also incorporates a process of regularization that helps in avoiding the issue of over-

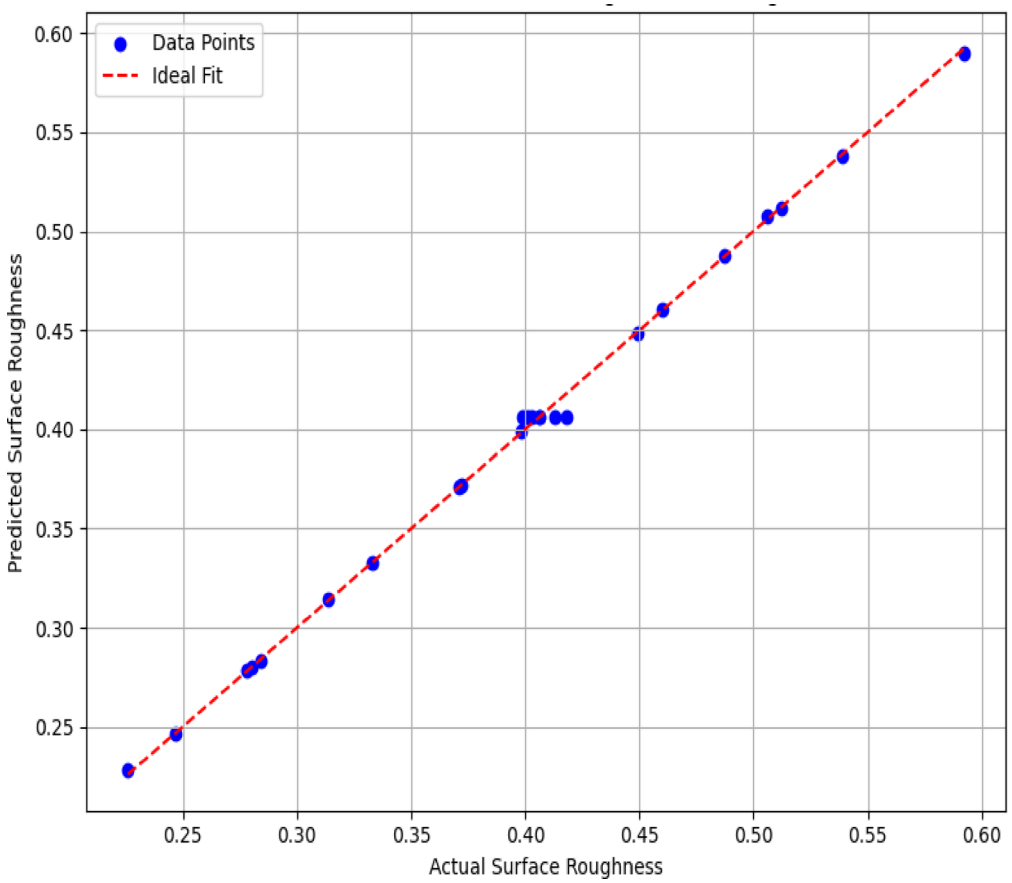

Fig. 6. Actual vs. predicted outcome variation from XGboost.

fitting. Such an approach guarantees the high efficiency and adaptability of the processes in the company. In RF, each tree works in parallel, and all the outcomes that are achieved are combined arithmetic mean. This makes this collaborative method more stable and accurate as compared to any other procedure that is followed. XGBoost optimizes explorative (searching through the hyperspace) and exploitive or refining ability better than random forest. This balance results in improvements in one's performance with many different datasets, including dental 3D printing datasets, especially when they are particularly intricate. Furthermore, both XGBoost and Random Forest give nearly accurate learnings of SR for the quality and accuracy of the dental devices being produced. This ensures that patients will get the best services and thus be satisfied with the services that were offered to them. Good predictions can be useful in enhancing 3D printing process settings as well as cutting the amount of time that is taken to finish the printed part due to poor surface finish. Random Sample Techniques give consistent and reliable predictions even in different batches and conditions, making the production of dental devices of high quality. This type of analysis allows for additional innovation of dental materials and 3D printing techniques – thanks to the use of advanced ML methods. Through the usage of ensemble techniques, the profession of dental practitioners is developed and enhanced resulting in better solutions for improving the dental field and beneficial services for patients. In comparison to the simple methods of modeling, there is a better performance of the ensemble methods such as XGB and RF in predicting the SR for direct 3D printing in the field of dentistry. These are fast and reliable since they merge the outcome of many decision trees to attain more reasonable convergence. Boosting is the final process where all the trees formed by the forest or each tree which may have been separately developed or built on a different data sample. This prevents overfitting and enhances the model's predictive accuracy when it is used in a different set of data. Because of their capacity to combine several models, lessen bias and variance, and perform subsequent iterations, they are highly efficient. Many advantages can be gained through these techniques for the dental practitioner that include increased predictive ability, ideal print result factors, and quality control, and in turn, an improvement in the delivery of dental health and treatment of patients. SVR employs kernel functions for capturing nonlinear behavior of the relationship. Despite that, it does not have a powerful error correcting feature that is witnessed in boosting methods such as XGBoost. It incorporates a broader search of the model space through the hyperparameters' optimization and regularization techniques. Cross-validation also adjusts the factor of model complexity in order to assure that the final model is as precise as it is general. Overfitting is a problem that affects the single decision trees, and ensemble method reduces this to a significantly low level. XGBoost reduces only the errors that are overlooked by the previous phase, and thus, it provides both bias and variance reduction sequentially. It is important to note that this two-step approach when error correcting will lead to improved models, where the first step corrects for

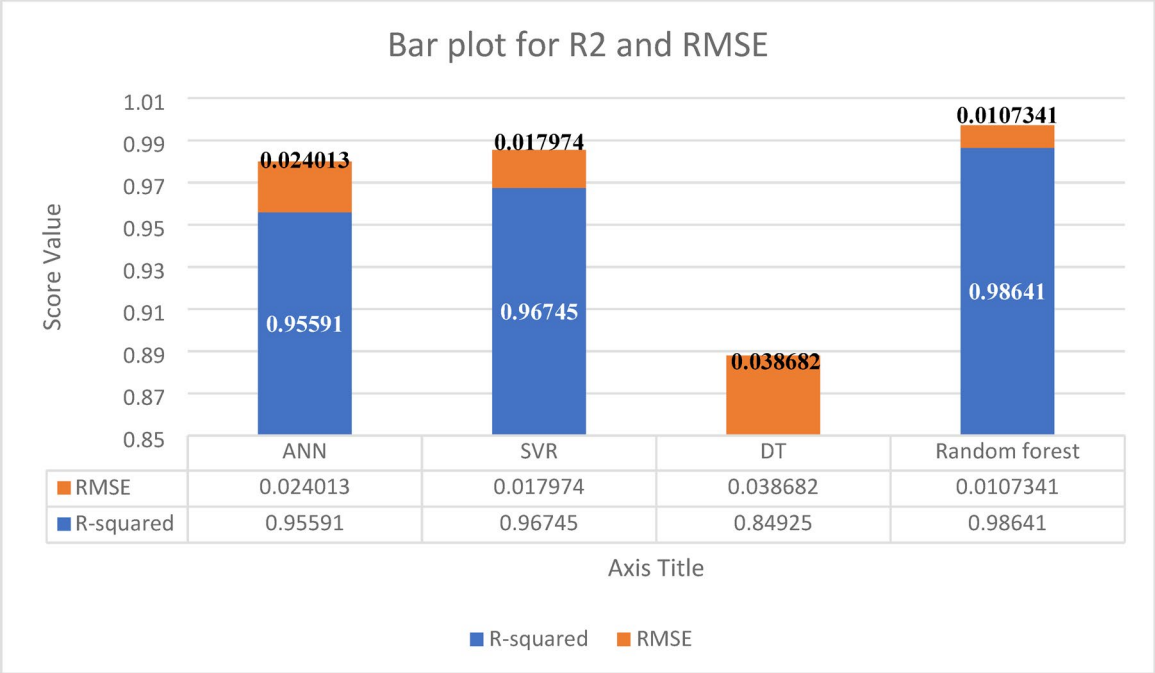

Fig. 7. Comparison among performance metrices.

bias, while the second corrects for variance. The higher accuracy portrayed by ensemble techniques especially the XGBoost was established due to its ability to use many models, rectifying wrong solutions in each step, and optimize both bias and variance. SVR, while strong among basic techniques due to its margin optimization and kernel trick, still falls short against the powerful collaborative and error-correcting mechanisms of ensemble methods. Similarly, ANN is effective in handling non-linear relationships, they lack the robust error-correction mechanisms inherent in ensemble methods. Figure 7 represents a comparison of results for various techniques. These advanced machine learning techniques provide several advantages over traditional methods, making them highly suitable for practitioners aiming to improve the quality and precision of dental devices.

Because they perform better, ensemble tactics are thus recommended. Ensemble effectively lowers variance and bias. For the exact specifications of dental 3D printing, the final model must be extremely accurate and generalised, which is ensured by this iterative error correction technique. For dental device quality management, precise SR forecasts are essential. Better patient results and satisfaction result from ensemble approaches, which guarantee that the printed surfaces fulfil the strict requirements needed in dentistry.

Conclusion

For dental direct 3D printing to produce high-quality implants and restorations, precise SR prediction is essential. This flexible framework has the potential to significantly outperform current optimisation techniques by providing more thorough optimisation, which would lead to substantial breakthroughs in AM technology. Additional clinical validation can boost its implicablity, where its limitation lies and can be explored in future extended work. Random Forest, XGBoost, and ensemble approaches perform better than simple modelling techniques according to performance measures. Ensemble approaches improve convergence and resilience by combining the predictions of several models. The use of ensemble is much more effective in terms of how many weak learners there are since they collectively work together. Ensembles reduce variance and bias. Random Forest has decrease in variance by taking averages while XGBoost reduces both bias and variance by boosting. Each model in the ensemble has its part in the decision made, which helps to reduce the effect oftrained on the model's errors. Employing it in this model increases the stability and, as a result, accuracy of values provided. It has been seen that our proposed SVR model outperforms ANN and DT but could not excel the ensemble techniques. In the case of SVR, there is no problem of overfitting, especially in the high dimensional space, where the aim is to identify a hyperplane that provides the highest margin between actual and expected values. SVR is superior to the basic approach of execution like Decision Trees in modelling complex patterns especially when non-linear interactions are involved through use of kernel functions. Since SVR may try different kernels, it can cope with different distributions of the given data and its complexity. Of the almost all the ensemble methods, XGBoost is superior to Random Forest. Thus, gradient boosting, which is used in XGBoost, builds models sequentially to correct errors made by previous models. A new and much tighter derivative model is developed due to this process of iteration. The method of regularisation is used in the XGBoost model to reduce model complexity and reduce high variance, which in another name for overfitting. XGBoost has a better design in terms of optimization factors like second gradient information and parallel computing to enhance the training speed and the model. Overall, XGBoost therefore makes better use of exploration vs. exploitation compared to

Random Forest especially when searching for better hyperparameters for different datasets while fine-tuning the current model. Thus, in the clinical application, to further increase the accuracy as well as the stability of models, using XGBoost and Random Forest, which are ensemble learning models, is significantly effective. Future work includes real-time control and in vivo validation would represent the next frontier in SR prediction and clinical implementation.

Data availability

The manuscript contains data that is used for the study. It cannot be provided for downloading because of the copyrights associated with it.

Received: 14 July 2025; Accepted: 25 August 2025
Published online: 01 September 2025

References

1. Srivastava, M. & Rathee, S. Optimisation of FDM process parameters by Taguchi method for imparting customised properties to components. *Virtual Phys. Prototyp.* **13**(3), 203–210 (2018).
2. Dhingra, A. K. et al. Driving design and performance of dental restorations through next-generation additive manufacturing resins. In *2024 3rd International Conference on Computational Modelling, Simulation and Optimization(ICCMSO)*, 344–349 (IEEE, 2024).
3. Kumar, A. & Chhabra, D. Multidisciplinary topology and material optimization approach for developing patient-specific limb orthosis using 3D printing. *Rapid Prototyp. J.* **29**(8), 1757–1771 (2023).
4. Srivastava, M., Rathee, S., Patel, V., Kumar, A. & Koppad, P. G. A review of various materials for additive manufacturing: recent trends and processing issues. *J. Mater. Res. Technol.* **21**, 2612–2641 (2022).
5. Pillai, S. et al. Dental 3D-printing: transferring art from the laboratories to the clinics. *Polymers* **13** https://doi.org/10.3390/polym13010157 (2021).
6. Yadav, M. et al. Enhancing dimensional accuracy of small parts through modelling and parametric optimization of the FDM 3D printing process using GA-ANN. In *2022 International Conference on Computational Modelling, Simulation and Optimization (ICCMSO)*, 89–94 (IEEE, 2022).
7. Kaushik, A. & Garg, R. K. Effect of printing parameters on the surface roughness and dimensional accuracy of digital light processing fabricated parts. *J. Mater. Eng. Perform.* (2023).
8. Magdy, N. M. et al. Evaluation of surface roughness of different direct resin-based composites. *J. Int. Soc. Prev. Community Dentistry*. **7**(3), 104–109 (2017).
9. Matos, G. R. M. Surface roughness of dental implant and osseointegration. *J. Oral. Maxillofac. Surg.* **20**(1), 1–4 (2021).
10. Sharma, A. & Bharti, P. S. Optimization of dlpprinting parameters for improved surface roughness using metaheuristic algorithms: A multifaceted approach. *J. Mater. Eng. Perform.* 1–15 (2024).
11. Vrochari, A. D. et al. Evaluation of surface roughness of ceramic and resin composite material used for conservative indirect restorations, after repolishing by intraoral means. *J. Prosthodont.* **26**(4), 296–301 (2017).
12. Albeshir, E. G. et al. Low-shrinkage resin matrices in restorative dentistry-narrative review. *Materials* **15**(8), 2951 (2022).
13. Da Silva, T. M. et al. Photosensitive resins used in additive manufacturing for oral application in dentistry: A scoping review from lab to clinic. *J. Mech. Behav. Biomed. Mater.* **141**, 105732 (2023).
14. Scotti, C. K. et al. Physical and surface properties of a 3D-printed composite resin for a digital workflow. *J. Prosthet. Dent.* **124**(5), 614–e1 (2020).
15. Alqutaibi, A. Y. et al. Polymeric denture base materials: A review. *Polymers* **15** https://doi.org/10.3390/polym15153258 (2023).
16. Erturk-Avunduk, A. T. et al. Effect of whitening concepts on surface roughness and optical characteristics of resin-based composites: an AFM study. *Microsc. Res. Tech.* **87**(2), 214–228 (2024).
17. Riva, Y. R. & Rahman, S. F. *Dental Composite Resin: A Review*. (AIP Publishing).
18. Al-Dulaijan, Y. A. et al. Comparative evaluation of surface roughness and hardness of 3D printed resins. *Materials* **15**(19), 6822 (2022).
19. V, M. Comparison of wear resistance of Hawley and vacuum formed retainers: an in-vitro study. *J. Dent. Biomaterials*. **3**, 248–253 (2016).
20. Leite, W. O. et al. Vacuum thermoforming process: an approach to modeling and optimization using artificial neural networks. *Polymers* **10**(2), 143 (2018).
21. Thurzo, A. et al. *Use of Optical Scanning and 3D Printing To Fabricate Customized Appliances for Patients with Craniofacial Disorders*. (Elsevier).
22. Sehrawat, S. et al. Study of 3D scanning technologies and scanners in orthodontics. *Mater. Today: Proc.* **56**, 186–193 (2022).
23. Tsolakis, I. A. et al. Three-Dimensional printing technology in orthodontics for dental models: A systematic review. *Children* **9** https://doi.org/10.3390/children9081106 (2022).
24. Tsoukala, E. et al. Direct 3D-printed orthodontic retainers. A systematic review. *Children* **10** https://doi.org/10.3390/children10040676 (2023).
25. Tsolakis, I. A. et al. Comparison in terms of accuracy between RESIN and LCD printing technology for dental model printing. *Dentistry J.* **10** https://doi.org/10.3390/dj10100181 (2022).
26. Koenig, N. et al. Comparison of dimensional accuracy between direct-printed and thermoformed aligners. *Korean J. Orthod.* **52**(4), 249–257 (2022).
27. Tack, P. et al. 3D-printing techniques in a medical setting: a systematic literature review. *Biomed. Eng. Online*. **15**(1), 115 (2016).
28. Sherman, S. L. et al. Accuracy of digital light processing printing of 3-dimensional dental models. *Am. J. Orthod. Dentofac. Orthop.* **157**(3), 422–428 (2020).
29. Ahangar, P. et al. Current biomedical applications of 3D printing and additive manufacturing. *Appl. Sci.* **9** https://doi.org/10.3390/app9081713 (2019).
30. Khalid, M. & Peng, Q. Investigation of printing parameters of additive manufacturing process for sustainability using design of experiments. *J. Mech. Des.* **143**(3) (2021).
31. Khorsandi, D. et al. 3D and 4D printing in dentistry and maxillofacial surgery: printing techniques, materials, and applications. *Acta Biomater.* **122**, 26–49 (2021).
32. Punia, U. et al. 3D printable biomaterials for dental restoration: A systematic review. *Mater. Today: Proc.* **63**, 566–572 (2022).
33. Lee, W. J. et al. Effect of build angle, resin layer thickness and viscosity on the surface properties and microbial adhesion of denture bases manufactured using digital light processing. *J. Dent.* **137**, 104608 (2023).
34. Li, J. et al. Multi-objective process parameters optimization of SLM using the ensemble of metamodels. *J. Manuf. Process.* **68**, 198–209 (2021).
35. Alhaddad, W. et al. Optimizing the material and printing parameters of the additively manufactured fiber-reinforced polymer composites using an artificial neural network model and artificial bee colony algorithm. *Structures* **46**, 1781–1795 (2022).

36. Hong, Q. et al. A direct slicing technique for the 3D printing of implicitly represented medical models. *Comput. Biol. Med.* **135**, 104534 (2021).
37. Yu, W., Nie, Z. & Lin, Y. Research on the slicing method with equal thickness and low redundancy based on STL files. *J. Chin. Inst. Eng.* **44**(5), 469–477 (2021).
38. Kumar, A. & Chhabra, D. Adopting additive manufacturing as a cleaner fabrication framework for topologically optimized orthotic devices: implications over sustainable rehabilitation. *Clean. Eng. Technol.* **10**, 100559 (2022).
39. McCarty, M. C. et al. Effect of print orientation and duration of ultraviolet curing on the dimensional accuracy of a 3-dimensionally printed orthodontic clear aligner design. *Am. J. Orthod. Dentofac. Orthop.* **158**(6), 889–897 (2020).
40. Lee, E. H. et al. Effect of post-curing time on the color stability and related properties of a tooth-colored 3D-printed resin material. *J. Mech. Behav. Biomed. Mater.* **126**, 104993 (2022).
41. Quan, H. et al. Photo-curing 3D printing technique and its challenges. *Bioactive Mater.* **5**(1), 110–115 (2020).
42. Ganta, G. K. et al. Clear aligners, the aesthetic solution: a review. *Int. J. Dent. Mater.* **3**(3), 90–95 (2021).
43. Abdulshahed, A. M. & Wafa, F. Surface roughness prediction in additive manufacturing: presenting the power of neural networks compared to linear regression. *J. Adv. Manuf. Syst.* 1–20 (2024).
44. McCarty, M. et al. Effect of print orientation and duration of ultraviolet curing on the dimensional accuracy of a 3-dimensionally printed orthodontic clear aligner design. *Am. J. Orthod. Dentofac. Orthop.* **158**, 889–897 (2020).
45. Ide, Y. et al. The effect of the angle of acuteness of additive manufactured models and the direction of printing on the dimensional fidelity: clinical implications. *Odontology* **105**, 108–115 (2017).
46. Ulkir, O., Bayraklılar, M. S. & Kuncan, M. Raster angle prediction of additive manufacturing process using machine learning algorithm. *Appl. Sci.* **14** https://doi.org/10.3390/app14052046 (2024).
47. Chen, H. et al. Concurrent build direction, part segmentation, and topology optimization for additive manufacturing using neural networks. *J. Mech. Des.* **145**(9) (2023).
48. Sahrir, C. D. et al. Effect of various post-curing light intensities, times, and energy levels on the color of 3D-printed resin crowns. *J. Dent. Sci.* **19**(1), 357–363 (2024).
49. Wu, D. et al. Mechanics of shape distortion of RESIN 3D printed structures during UV post-curing. *Soft Matter*. **15**(30), 6151–6159 (2019).
50. Türker, H., Aksoy, B. & Özsoy, K. Fabrication of customized dental guide by stereolithography method and evaluation of dimensional accuracy with artificial neural networks. *J. Mech. Behav. Biomed. Mater.* **126**, 105071 (2022).
51. Rojek, I. et al. Traditional artificial neural networks versus deep learning in optimization of material aspects of 3D printing. *Materials* **14** https://doi.org/10.3390/ma14247625 (2021).
52. Mahmood, M. A. et al. Artificial neural network algorithms for 3D printing. *Materials* **14** https://doi.org/10.3390/ma14010163 (2021).
53. Special issue: machine learning for engineering design. *J. Mech. Des.* **141**(11) (2019).
54. Wu, D., Wei, Y. & Terpenny, J. Predictive modelling of surface roughness in fused deposition modelling using data fusion. *Int. J. Prod. Res.* **57**(12), 3992–4006 (2019).
55. Sachdeva, I. et al. Computational AI models in VAT photopolymerization: a review, current trends, open issues, and future opportunities. *Neural Comput. Appl.* **34**(20), 17207–17229 (2022).
56. Chinchanikar, S. et al. ANN modelling of surface roughness of FDM parts considering the effect of hidden layers, neurons, and process parameters. *Adv. Mater. Process. Technol.* **10**(1), 22–32 (2024).
57. Prasad, J. et al. Machine learning predictive model as clinical decision support system in orthodontic treatment planning. *Dentistry J.* **11** https://doi.org/10.3390/dj11010001 (2023).
58. Agarwal, R., Singh, J. & Gupta, V. A data-driven ensemble machine learning approach for predicting the mechanical strength of 3D printed orthopaedic bone screws. *Proc. Inst. Mech. Eng. Part E J. Process Mech. Eng.* 09544089231211235 (2023).
59. Asselman, A., Khaldi, M. & Aammou, S. Enhancing the prediction of student performance based on the machine learning XGBoost algorithm. *Interact. Learn. Environ.* **31**(6), 3360–3379 (2023).
60. Lin, L. et al. 3D printing and digital processing techniques in dentistry: a review of literature. *Adv. Eng. Mater.* **21**(6), 1801013 (2019).
61. Dimiduk, D. M., Holm, E. A. & Niezgoda, S. R. Perspectives on the impact of machine learning, deep learning, and artificial intelligence on materials, processes, and structures engineering. *Integrating Mater. Manuf. Innov.* **7**(3), 157–172 (2018).
62. Punia, U. & Garg, R. K. Enhancing mechanical performance of 3D printable PMMA resin through strategic incorporation of SS 316 L nanoparticles for dental applications. *Int. J. Interact. Des. Manuf.* **18**, 6317–6332. https://doi.org/10.1007/s12008-024-02036-1 (2024).
63. Singh, R. K. et al. A novel hybridization of artificial neural network and moth-flame optimization (ANN–MFO) for multi-objective optimization in magnetic abrasive finishing of aluminium 6060. *J. Brazilian Soc. Mech. Sci. Eng.* **41**, 1–19 (2019).
64. Kopper, A. et al. Model selection and evaluation for machine learning: deep learning in materials processing. *Integrating Mater. Manuf. Innov.* **9**(3), 287–300 (2020).
65. Xie, Y. et al. A backpropagation neural network improved by a genetic algorithm for predicting the mean radiant temperature around buildings within the long-term period of the near future. *Build. Simul.* **15**(3), 473–492 (2022).
66. Demirbay, B., Kara, D. B. & Uğur, Ş. Multivariate regression (MVR) and different artificial neural network (ANN) models developed for optical transparency of conductive polymer nanocomposite films. *Expert Syst. Appl.* **207**, 117937 (2022).
67. Bardak, S. et al. Predictive performance of artificial neural network and multiple linear regression models in predicting adhesive bonding strength of wood. *Strength Mater.* **48**(6), 811–824 (2016).
68. Nagarajan, H. P. N. et al. Knowledge-Based design of artificial neural network topology for additive manufacturing process modeling: A new approach and case study for fused deposition modeling. *J. Mech. Des.* **141**(2) (2018).
69. Gupta, A. K. & Taufik, M. Investigation of dimensional accuracy of material extrusion build parts using mathematical modelling and artificial neural network. *Int. J. Interact. Des. Manuf. (IJIDeM)*. **17**(2), 869–885 (2023).
70. Kabengele, K. T., Tartibu, L. K. & Olayode, I. O. *Analysis of 3D Printing Performance Using Machine Learning Techniques*. (American Society of Mechanical Engineers).
71. Goh, G. D., Sing, S. L. & Yeong, W. Y. A review on machine learning in 3D printing: applications, potential, and challenges. *Artif. Intell. Rev.* **54**(1), 63–94 (2021).
72. Awad, M. et al. *Support vector regression*. Efficient learning machines: Theories, concepts, and applications for engineers and system designers, 67–80 (2015).
73. Cerro, A. et al. Use of machine learning algorithms for surface roughness prediction of printed parts in Polyvinyl butyral via fused deposition modeling. *Int. J. Adv. Manuf. Technol.* **115**(7), 2465–2475 (2021).
74. Suthaharan, S. & Suthaharan, S. *Support vector machine*. Machine learning models and algorithms for big data classification: thinking with examples for effective learning, 207–235 (2016).
75. Yang, Y. et al. Optimization of polylactic acid 3D printing parameters based on support vector regression and cuckoo search. *Polym. Eng. Sci.* **63**(10), 3243–3253 (2023).
76. Montesinos López, O. A., Montesinos, A., López & Crossa, J. *Support Vector Machines and Support Vector Regression, in Multivariate Statistical Machine Learning Methods for Genomic Prediction*, 337–378 (Springer, 2022).
77. Rizal, N. M. Comparison between regression models, support vector machine (SVM), and artificial neural network (ANN) in river water quality prediction. *Processes*. **10** https://doi.org/10.3390/pr10081652 (2022).

78. Akbari, P., Zamani, M. & Mostafaei, A. Machine learning prediction of mechanical properties in metal additive manufacturing. *Additive Manuf.* **91**, 104320 (2024).
79. Ferdous, J. et al. Development of a generic decision tree for the integration of Multi-Criteria Decision-Making (MCDM) and Multi-Objective optimization (MOO) methods under uncertainty to facilitate sustainability assessment: A methodical review. *Sustainability* **16**(7), 2684 (2024).
80. Sirocchi, C., Bogliolo, A. & Montagna, S. Medical-informed machine learning: integrating prior knowledge into medical decision systems. *BMC Med. Inf. Decis. Mak.* **24**(4), 186 (2024).
81. Talaat, F. M. & Hassan, E. *Artificial Intelligence in 3D Printing*. (Springer).
82. Barrios, J. M. & Romero, P. E. Decision tree methods for predicting surface roughness in fused deposition modeling parts. *Materials* **12**(16), 2574 (2019).
83. Zhang, X. et al. Machine learning-driven 3D printing: A review. *Appl. Mater. Today*. **39**, 102306 (2024).
84. Priyanka & Kumar, D. Decision tree classifier: a detailed survey. *Int. J. Inform. Decis. Sci.* **12**(3), 246–269 (2020).
85. Sharma, P. et al. Predicting the dimensional variation of geometries produced through FDM 3D printing employing supervised machine learning. *Sens. Int.* **3**, 100194 (2022).
86. Wu, D., Wei, Y. & Terpenny, J. *Surface Roughness Prediction in Additive Manufacturing Using Machine Learning*. (American Society of Mechanical Engineers).
87. Jayasudha, M. et al. Accurate estimation of tensile strength of 3D printed parts using machine learning algorithms. *Processes* **10**(6), 1158 (2022).
88. Chowdhury, D., Sinha, A. & Das, D. XAI-3DP: Diagnosis and understanding faults of 3-D printer with explainable ensemble AI. *IEEE Sens. Lett.* **7**(1), 1–4 (2022).
89. Dabbagh, S. R., Ozcan, O. & Tasoglu, S. Machine learning-enabled optimization of extrusion-based 3D printing. *Methods* **206**, 27–40 (2022).
90. Ege, D. et al. Machine learning models to predict the relationship between printing parameters and tensile strength of 3D Poly (lactic acid) scaffolds for tissue engineering applications. *Biomedical Phys. Eng. Express*. **9**(6), 065014 (2023).
91. Mishra, A. et al. Explainable artificial intelligence (XAI) and supervised machine learning-based algorithms for prediction of surface roughness of additively manufactured polylactic acid (PLA) specimens. *Appl. Mech.* **4**(2), 668–698 (2023).
92. Chakraborty, S. & Bhattacharya, S. Application of XGBoost algorithm as a predictive tool in a CNC turning process. *Rep. Mech. Eng.* **2**(1), 190–201 (2021).

Acknowledgements

1. The authors thank the King Khalid University for the financial support.2. The author is grateful to DCRUST University in Murthal in Haryana for offering the experimental facilities.

Author contributions

Conceptualization and Methodology: Anmol Sharma, Ravinder SainiData Curation and Formal Analysis: Vishwanath Gurumurthy, Ashish KaushikValidation and formal analysis: Artak HeboyanInvestigation and Resources: Anmol SharmaOriginal draft preparation: Rajesh Vyas Rayan Ibrahim BinduhayyimWriting, Reviewing, and Editing: Mohamed Saheer, Artak Heboyan, Supervision and Project Administration: Ravinder Saini, Artak HeboyanFunding Acquisition: Mohamed Saheer. Funding Acquisition: Mohamed Saheer.

Funding

The authors extend their appreciation to the Deanship of Research and Graduate Studies at King Khalid University for funding this work through Large Research Project under grant number RGP2/633/46.

Declarations

Competing interests

The authors declare no competing interests.

Additional information

Correspondence and requests for materials should be addressed to A.H.

Reprints and permissions information is available at www.nature.com/reprints.

Publisher's note Springer Nature remains neutral with regard to jurisdictional claims in published maps and institutional affiliations.